Neuroelectromagnetic signatures of the reproduction of supra-second durations

Kononowicz, Tadeusz W.; Sander, Tillman; van Rijn, Hedderik

Published in:
Neuropsychologia

DOI:
10.1016/j.neuropsychologia.2015.06.001

Neuropsychologia 75 (2015) 201–213

Contents lists available at ScienceDirect

Neuropsychologia

journal homepage: www.elsevier.com/locate/neuropsychologia

Neuroelectromagnetic signatures of the reproduction of supra-second durations

Tadeusz W. Kononowicz [a,b,*], Tillman Sander [c], Hedderik van Rijn [a,**]

[a] Experimental Psychology, University of Groningen, Groningen, The Netherlands
[b] CEA, DSV/I2BM, NeuroSpin; INSERM, Cognitive Neuroimaging Unit, U992; Université Paris-Sud, Gif-sur-Yvette, France
[c] Physikalisch-Technische Bundesanstalt, Berlin, Germany

ARTICLE INFO

Article history:
Received 8 March 2015
Received in revised form
6 May 2015
Accepted 1 June 2015
Available online 6 June 2015

Keywords:
Contingent negative variation
Contingent magnetic variation
Magnetic fields
Supplementary motor area
Interval timing
Climbing neural activity

ABSTRACT

When participants are asked to reproduce an earlier presented duration, EEG recordings typically show a slow potential that develops over the fronto-central regions of the brain and is assumed to be generated in the supplementary motor area (SMA). This contingent negative variation (CNV) has been linked to anticipation, preparation and formation of temporal judgment (Macar, Vidal, and Casini, 1999, *Experimental Brain Research*, 125(3), 271–80). Although the interpretation of the CNV amplitude is problematic (Kononowicz and Van Rijn, (2011), *Frontiers in Integrative Neuroscience*, 5(48); Ng, Tobin, and Penney, 2011, *Frontiers in Integrative Neuroscience*, 5(77)), the observation of this slow potential is extremely robust, and thus one could assume that magnetic recordings of brain activity should show similar activity patterns. However, interval timing studies using durations shorter than one second did not provide unequivocal evidence as to whether CNV has a magnetic counterpart (CMV). As interval timing has been typically associated with durations longer than one second, participants in this study were presented intervals of 2, 3 or 4 s that had to be reproduced in setup similar to the seminal work of Elbert et al. (1991, *Psychophysiology*, 28(6), 648–55) while co-recording EEG and MEG.

The EEG data showed a clear CNV during the standard and the reproduction interval. In the reproduction interval the CNV steadily builds up from the onset of interval for both stimulus and response locked data. The MEG data did not show a CNV-resembling ramping of activity, but only showed a pre-movement magnetic field (preMMF) that originated from the SMA, occurring approximately 0.6 s before the termination of the timed interval. These findings support the notion that signatures of timing are more straightforwardly measured using EEG, and show that the measured MEG signal from the SMA is constrained to the end of reproduction interval, before the voluntary movement.

Moreover, we investigated a link between timing behavior and the early iCNV and late CNV amplitudes to evaluate the hypothesis that these amplitudes reflect the accumulation of temporal pulses. Larger iCNV amplitudes predicted shorter reproduced durations. This effect was more pronounced for the 2 s interval reproduction, suggesting that preparatory strategies depend on the length of reproduced interval. Similarly to Elbert et al. (1991, *Psychophysiology*, 28(6), 648–55), longer reproductions were associated with smaller CNV amplitudes, both between conditions and across participants within the same condition. As the temporal accumulation hypothesis predicts the inverse, these results support the proposal by Van Rijn et al. (2011, *Frontiers in Integrative Neuroscience*, 5) that the CNV reflects other temporally driven processes such as temporal expectation and preparation rather than temporal accumulation itself.

1. Introduction

The most well-known electrophysiological marker of interval timing is the contingent negative variation (CNV), a fronto-central negative potential in the encephalogram building up until a temporally predictable stimulus has been presented (Walter et al., 1964) or a temporal decision has been made (e.g., Macar and Vidal, 2003; Ng et al., 2011; Wiener et al., 2012). Although the CNV is

* Corresponding author at: CEA.DSV.I2BM.NeuroSpin – INSERM Cognitive Neuroimaging Unit, Bât 145 Point Courrier 156, Gifs/Yvette F-91191, France.
** Corresponding author at: Experimental Psychology, Grote Kruistraat 2/1, 9712 TS Groningen, The Netherlands.
E-mail addresses: t.w.kononowicz@icloud.com (T.W. Kononowicz), Tilmann.Sander-Thoemmes@ptb.de (T. Sander), hedderik@van-rijn.org (H. van Rijn).

http://dx.doi.org/10.1016/j.neuropsychologia.2015.06.001

widely recognized as a signature of the processes involved in interval timing Elbert et al., 1991; Macar and Vidal, 2004; Walter et al., 1964; Ruchkin et al., 1977), both in the context of short (e.g., < 1 s) and longer (> 1 s) intervals, the CMV, the magnetic counterpart of the CNV, has not received much attention. Work that has compared the CNV and CMV (e.g., N'Diaye et al., 2004), suggests that these measures reflect different properties of interval timing tasks. For example, while EEG studies have shown that the SMA is the main source contributing to the CNV (e.g., Gómez et al., 2007), the status of this structure with respect to magnetic activity has not been settled (N'Diaye et al., 2004; Gómez et al., 2004). As previous CMV studies focused on short intervals, which are often considered to be different from longer intervals (e.g., Lewis and Miall, 2003; Rammsayer, 1999), we investigated slow electric potentials and magnetic fields related to supra-second interval timing by co-recording magnetic and electric brain signals. To allow for a precise comparison between CNV and CMV, we based our experiment on two classical studies that used a time reproduction paradigm in which a number of supra-second durations are used (Elbert et al., 1991; Gibbons and Rammsayer, 2004). Presenting participants with a number of different durations will allow us to address the question whether electromagnetic field power indexes the reproduced duration.

The CNV has been related to several processes such as anticipation (Tecce, 1972) or preparation for sensory information processing (e.g., Boehm et al., 2014; Brunia and van Boxtel, 2001; Elbert and Rockstroh, 1987; O'Connell et al., 2009). Two subcomponents can be identified in the CNV (Loveless and Sanford, 1974): the initial iCNV and the terminal tCNV (often referred to as the CNV, a term we will also use in this document). The iCNV has been associated with an orienting response (e.g., Bender et al., 2004; Fischer et al., 2008; Simons et al., 1979) or early anticipation processes (e.g., Fischer et al., 2010; Lütcke et al., 2009) whereas the tCNV has been linked to motor preparation (e.g., Loveless and Sanford, 1974) or anticipation processes (e.g., Boehm et al., 2014).

As the CNV can also be found in a variety of tasks in which a temporal contingency between two relevant stimuli exists, it has been associated with the processing of temporal intervals. For example, influential studies by Elbert et al. (1991) and Gibbons and Rammsayer (2004) showed that slow cortical potentials measured during supra-second durations can be used to track processes involved in both perception and reproduction of temporal intervals. As the development of the CNV during a trial aligns with the conceptual construct of the accumulation of time (see Van Rijn et al., 2014, for a review of theories based on this conceptualization) or, more general, the notion of climbing neuronal activity (CNA), many interval timing studies have focused on the role of the CNV in interval timing tasks (e.g., Macar and Vidal, 2009, but see Van Rijn et al. (2011), for arguments against this connection).

Although the CNV is correlated with activity in a wide variety of cortical structures (e.g., ACC, M1, and medial frontal gyrus; Gómez et al., 2007', 2003; Mento et al. (2014); Scheibe et al., 2010), the primarily active structure is the supplementary motor area (SMA, e.g., Gómez et al., 2007', 2003; Liu, et al., 2013; Mento et al., 2013; Nagai et al., 2004; Pouthas et al. 2000; Leuthold et al. 2004, cf., Praamstra et al., 2006). This aligns with the central role assumed for the SMA in theories explaining preparatory and intentional processes (for a review see Haggard (2008), Nachev et al., (2008), Penfield and Welch, 1951, Tanji, (1994) and see also Boehm et al. (2014)), and interval timing (e.g., Bueti and Macaluso, 2011; Coull et al., 2004; Wiener et al., 2010). It is therefore important to provide converging evidence for the central role of the SMA in CNA. As electroencephalographic (EEG) and magnetoencephalographic (MEG) signals are measured from differently oriented pyramidal cells (e.g., Hämäläinen et al., 1993), magnetic fields and electric potentials provide complementary sources of information regarding brain function (Coull 2009; Hari et al., 2000). In the context of foreperiod paradigms, in which timing is secondary to the primary instruction to respond as quickly as possible to an imperative stimulus, several studies using MEG have observed a magnetic counterpart of the CNV that was termed the contingent magnetic variation (CMV; Basile et al., 1994; Dammers and Ioannides, 2000; Elbert et al., 1994; Gómez et al., 2004; Hultin et al., 1996; Vieth et al., 1991). However, MEG studies on the Bereitschaftspotential have shown that the slow buildup that is typically measured with EEG might be difficult to detect with MEG (see Erdler et al., 2000) as the SMA is active bilaterally, and the closely located but opposing dipoles might cancel each other out.

Although most neuroelectromagnetic work in the interval timing field has focused on CNV activity and the CMV has largely been neglected, notable exceptions are the studies by N'Diaye et al. (2004), by Sieroka et al. (2003), by Noguchi and Kakigi (2006), and recent study by van Wassenhove and Lecoutre (2015). N'Diaye at al. (2004) co-recorded EEG and MEG during an interval discrimination task with filled durations shorter than one second. In line with the results discussed above, the CNV was shown to originate from mid-frontal structures, but source reconstructions of sustained auditory magnetic fields did not show any activation coming from mid-frontal structures such as the SMA. As the intersection of the sources for EEG and MEG mainly involved sensory and supra-modal associative regions, N'Diaye et al. (2004) suggested that interval timing largely depends on these regions. A similar lack of observed involvement of the SMA is reported in the work of Sieroka et al. (2003), as they identified the posterior cingulate gyrus as the source of slow magnetic fields observed during the perception of 1.4 s intervals, and by the MEG study of Gómez et al. (2004) in which no involvement of the SMA was found in a foreperiod paradigm. Offsetting the studies that did not find evidence for the involvement of the SMA, Noguchi and Kakigi (2006) showed that magnetic activity in the SMA increased during the perception of intervals shorter than 1 s. This incongruity could partly be accounted for by the different responding regimes that were employed. In the study by Noguchi and Kakigi (Noguchi, 2014, personal information) study, participants always responded with their right thumb, whereas either with the right or left thumb in the study of N'Diaye et al. (2004). As previous EEG work (e.g., Ulrich et al., 1998) has shown that recorded amplitude increases as a function of the amount of advance information regarding the required movement, it might have been more difficult to measure any SMA-based activity in studies in which responses have to be given by either the left or right hand. An alternative explanation is that restricting responses to the right hand might have resulted in a larger difference in left and right SMA dipole activity, making it possible to pick up SMA activity as the asymmetry in dipole activity prevents a complete canceling out of the signal.

Interestingly, all these studies used fairly short intervals (i.e., < = 1.4 s), whereas interval timing is typically considered to be as ranging from the short intervals tested in these studies to longer intervals lasting up to, at least, a couple of seconds (e.g., Buhusi and Meck, 2005; Gallistel and Gibbon, 2000). One of the reasons why previous studies might have been limited to shorter time intervals is that measurement of slow potentials, especially when measuring MEG, can be contaminated by various environmental and physiological factors. Moreover, measuring longer durations are intrinsically associated with higher noise levels and special care has to be taken with respect to the recording procedure (Mackert et al., 1999; Sander et al., 2009).

Given the unequivocal results regarding the cortical origins and the contribution of magnetic fields to supra-second time estimation and the lack of robust information on the potential differential contribution of slow electric and magnetic fields to the perception

and production of supra-second intervals, we assessed the role of the CNV and the CMV in a time reproduction paradigm similar to that of Elbert et al. (1991) and Gibbons and Rammsayer (2004). In these studies, participants were asked to perceive non-filled supra-second intervals of different durations presented in random order, and to reproduce the durations after perceiving them. This design allows for the assessment of the role of slow electromagnetic waves during the pure perceptual stage and the reproduction stage (see Wiener et al. (2012)), and thus for assessing which neuronal populations contribute to the slowly evolving activity in the various stages of the interval timing task. Moreover, by presenting participants with different durations, we can address whether the observed field power is a function of the reproduced duration. This issue, which will be more extensively addressed in the discussion, is central to the functional role of climbing neuronal activity in interval timing (Kononowicz and Van Rijn, 2011, 2014; Macar et al., 1999; Ng et al., 2011; Van Rijn et al., 2011; Wiener et al., 2012), and to the role of the SMA in decision making (e.g., Boehm et al., 2014).

2. Method

2.1. Participants

Eighteen students enrolled at the Humboldt, Freie or Technical University of Berlin with no self-reported hearing/vision loss or neurological pathology took part in the experiment and received monetary compensation for participation. Informed consent as approved by the Ethical Committee Psychology of the University of Groningen was obtained before testing. The data of one participant were not included in the analyses as he fell asleep during the experiment. The final sample comprised data of 17 participants (all right handed, 8 males). All cells of the design contained at least 30 observations.

2.2. Stimuli and procedure

Fig. 1 depicts the time course of one trial. Each trial started with the presentation of a "+" sign. After a randomly sampled duration (either 2.5, 3.5 or 4.5 s), the standard interval (SI) was presented by means of two tone bursts (5 ms, 1 kHz, ~75 dB) either 2, 3 or 4 s apart. The "+" remained on the screen during the presentation of the SI and remained on the screen for either 1.5 or 2.5 s after the SI, after which the reproduction interval (RI) started. The start of the RI was signaled by another tone burst and a change of the fixation character to an "x". Participants were instructed to press the mouse button with their right hand when they thought the "x" was on the screen for the same amount of time as the just presented standard interval. Pressing the mouse button initiated the offset tone burst, and the "x" was removed from the screen. After an inter-trial interval (either 1.5 or 2.5 s, randomly sampled) the next trial started. Each of the three SI durations was presented 40 times. The 120 trials were presented in blocks of 10 trials, each block containing at least 3 repetitions of each SI in randomized order. Between blocks, participants got adaptive feedback on their performance indicating how many trials were responded to correctly. The range of correct feedback was initially set to 20% deviation of the target interval. This range was dynamically adjusted by decreasing (2.5%) or increasing (0.5%) the range after each correct or incorrect trial, respectively. Participants were asked to reproduce the durations as accurately as possible and maximize number of correct trials in each block. Before the experimental trials started, participants were presented five practice trials.

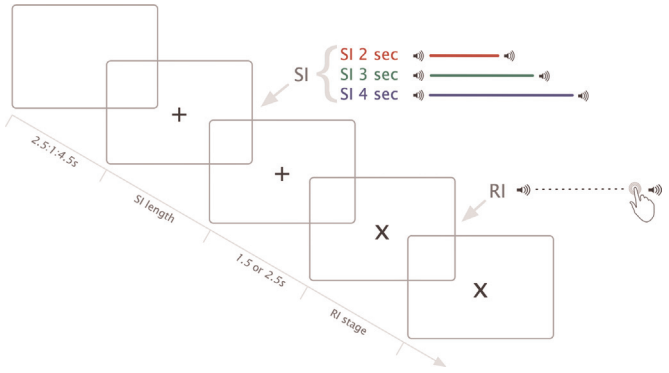

Fig. 1. Time course of the experimental trials in the time reproduction task.

2.3. Simultaneous MEG–EEG recordings

In a dimly-lit, standard magnetically-shielded room (Ak3b, Vacuumschmelze, Hanau, Germany) located at the PTB Berlin, each participant lay horizontally with eyes open looking at a screen that was used to present visual stimuli using a projector located outside of the magnetically shielded room. Participants were asked to cross their arms in front of their chest, as earlier work has shown this position to be most comfortable during longer recording sessions, and to respond by clicking a button on a computer mouse which was held in the right hand, but was located at their left upper body. Measurements were carried out with a Yokogawa MEG system (Yokogawa Electric Corporation, Japan), containing 125 axial gradiometers and three reference magnetometers. Electrical brain activity was measured with a custom-built low noise biosignal amplifier (PTB, unpublished, Scheer, 2006). Both EEG and MEG signals were recorded with a sampling rate of 500 Hz. EEG signal was recorded from 30 scalp locations using Ag–AgCl electrodes (EasyCap, Germany), with impedances kept below 5 kΩ. Vertical and horizontal EOG activity and both mastoids were registered.

The head position with respect to the sensor helmet was measured using coils attached to the scalp at anatomical landmarks (nasion and preauricular points). The locations of the coils and EEG electrode positions were digitized with respect to three anatomical landmarks with a 3D digitizer (Zebris, Isny, Germany).

The brief auditory bursts indicating the start and end of the intervals were presented binaurally via MEG-compatible tube earphones (Etymotic research, Elk Grove Village, USA) at sound levels set for each participant individually, but was generally at about 75 dB. Stimuli were presented using a PC running Presentation software (Neurobehavioral Systems).

3. Data analysis

The data were analyzed using FieldTrip (Oostenveld et al., 2011; version 20130713) and custom written Matlab code. The MEG data was denoised by computing noise cancelation weights using three reference channels. First, PCA was computed on the reference channels and then projected to the gradiometer channels and subtracted from the data of interest. This computation was performed separately for each trial using FieldTrip's *ft_denoise_pca* function. A 50 Hz notch filter and a bandpass FIR filter (0.01–130 Hz) were applied to the EEG and MEG data. Trials containing excessive ocular artifacts, movement artifacts, amplifier saturation, or SQUID artifacts were selected by visual inspection and excluded from further processing. Eye blinks, heart beat, and muscle artifacts were corrected using Independent Component Analysis (Bell and Sejnowski, 1995). As we were interested in slow shifts of activity (see also N'Diaye et al. (2004)), EEG and MEG data were

filtered with a lowpass 7 Hz FIR filter prior to averaging and baselined to the average activity calculated over 200 ms preceding the tone onset. The 7 Hz filtered data were used for all subsequent analyses. The MEG data were not spatially realigned prior to the averaging, thus EEG-like averages were obtained for the sensor space data.

All analyses of brain imaging data focused on the amplitude of slow components using non-parametric cluster-based permutation tests which controls for multiple comparisons (Maris and Oostenveld, 2007), based on two-sided Hotteling's T^2 and MANOVA dependent sample *F*-tests test using FieldTrip's default methods. This analysis method allows us to include all electrodes into analysis instead of having to predefine a particular subset of electrodes as is typically done in CNV research. Apart from the obvious advantage that this reduced the risk of an outcome driven by a confirmation bias, it also allows us to keep EEG and MEG analyses as similar and consistent as possible. The permutation distribution was approximated by drawing 1000 random permutations of the observed data. The *p* values are informative about the null hypothesis that the probability distribution of the condition-specific averages is independent of the conditions. For all cluster-based analyses we averaged data over indicated time intervals, but did not average over the channel dimension, allowing us to identify significant clusters of neighboring electrodes or sensors (neighbor configuration was based on Fieldtrip's default EEG 10-10 neighbor template). As mentioned, the cluster-based analysis differs from most CNV analyses, as these are often based on an ANOVA-driven analysis of a subset of electrodes. However, to allow for the comparison with earlier work, we follow a more typical approach for the visualization of the EEG data as we plotted all effects for predefined clusters based on earlier literature (e.g., Ng et al., 2011; Verleger et al., 2000). As the MEG data analysis is more exploratory and we did not want to commit to specific regions, we used dynamic criteria based on maximum amplitudes in a certain time range to select the data for visualization.

Earlier work by Elbert et al. (1991) or Gibbons and Rammsayer (2004) assessed the CNV during the RI based on stimulus-locked data (RI_{SL}). However, as the reproduced durations follow a relative wide distribution, we assess the buildup during the later parts of the reproduction on the response-locked data (RI_{RL}). Obviously, for the initial-CNV/initial-CMV (iCNV/iCMV) effects, RI_{SL} data will be used. Following earlier work, the last 500 ms before the response were used for the response locked CNV/CMV data (Gibbons and Rammsayer, 2004; Gibbons and Stahl, 2008). To assess the iCNV and iCMV components, we focused on the 300 ms time window ranging from 0.3 to 0.6 s after the onset of the duration. All between-condition CNV/CMV statistics for the stimulus locked EEG and MEG data (RI_{SL}) are based on the 500 ms time interval ranging from 1.5 to 2 s after the onset of the duration.

3.1. Source reconstruction

As 26 electrodes are not sufficient for reliable source reconstructions, we refrained from reconstruction analyses based on EEG data, and only present source reconstructions for the MEG data. Each participant's head position was realigned with respect to SQUID sensors using the digitalized anatomical landmarks. For group statistics and for illustrative purposes, source activities were projected onto a standard Montreal Neurological Institute brain (FieldTrip/SPM8). The forward solution for the MEG data was calculated using a semi-realistic single shell model (Nolte, 2003). The source model was computed with 9 mm resolution. Finally, lead field matrices corresponding to the two tangential orientations were computed for each grid point.

For source reconstructions we used a spatial filtering based on linearly constrained minimum variance beamformer (LCMV, Van Veen et al., 1997) as implemented by FieldTrip. The covariance matrices of the unaveraged single trial data were computed for the corresponding time windows. Subsequently, these covariance matrices and lead fields were used to compute the coefficients of spatial filters for each grid point in the source model. The neural activity index (NAI, Van Veen et al., 1997) was determined by normalizing the activity in the window of interest with noise estimated directly from the data by obtaining the smallest singular value of singular value decomposition. This analysis provided us with noise-normalized estimates of source power derived from beamformer filters, termed as pseudo-*z* (Robinson and Vrba, 1999) or as NAI (Van Veen et al., 1997). Activity in each grid point was projected to its strongest orientation. To investigate neural sources driving CMV signals we followed the procedure presented by Gomez et al., (2003), meaning that NAI values were normalized for each subject using *z*–score statistics and the source reconstructions were averaged over subjects. To prevent smearing of *z*-values, prior to visualization, these averaged reconstructions were *z*-transformed again. For visualization of the sources of magnetic activity we used the values that exceeded one standard deviation, which corresponds to the threshold utilized in Gómez et al. (2003).

We applied the LCMV method as, despite some theoretical caveats, it has been successfully utilized in many paradigms investigating phase locked responses (e.g., Hillebrand et al., 2005; Darvas et al., 2004). Moreover, LCMV beamformer has been successfully used in the localization of signals from the bilateral auditory cortices (Todorovic et al., 2011), anterior cingulate cortex (Keil et al., 2010) and it has been successfully applied to slow premovement magnetic fields originating from bilateral premotor structures (Cheyne et al., 2006).

4. Results

4.1. Behavioral results

Fig. 2 shows the density functions of all time reproductions for each condition. The three separate peaks signify that participants did distinguish between the temporal intervals. The 3 s and 4 s conditions were clearly underestimated which is confirmed by *t*-tests against target duration [3 s, $t(16)=4.2$, $p<0.001$; 4 s: $t(16)=5.4$, $p<0.001$]. Numerically, the 2 s condition was slightly overestimated, but not different from 2 s ($t<1$). Underestimation of

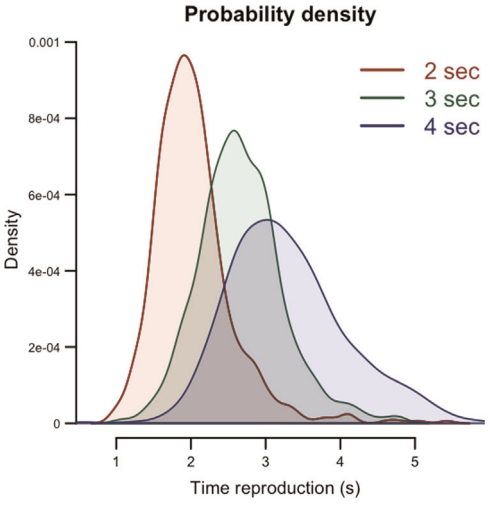

Fig. 2. Probability density functions (Sheather and Jones, 1991) of time reproductions plotted for the three conditions separately.

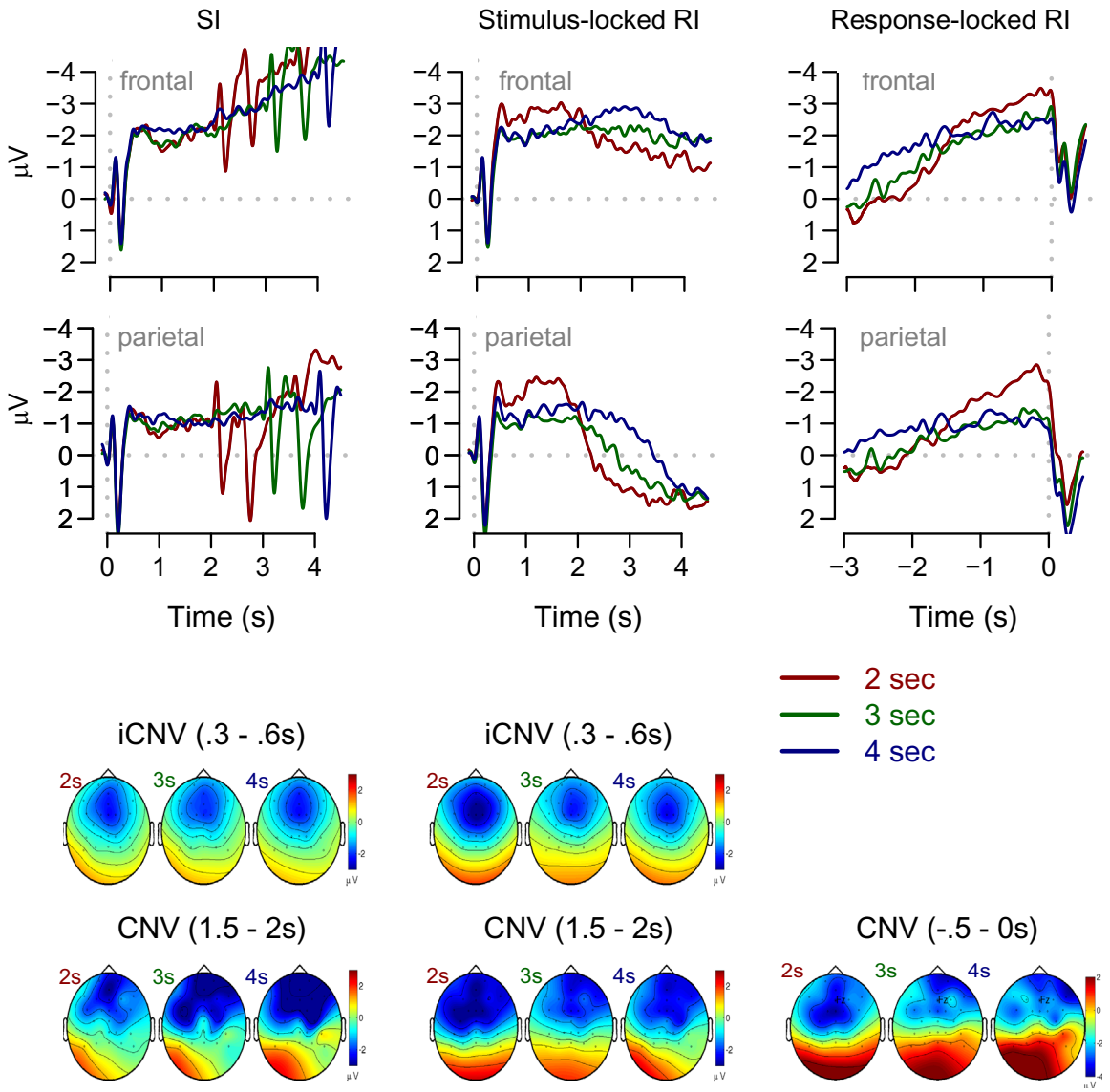

Fig. 3. Sensor-space results for the EEG data: top panel reflects (i) CNV time courses during SI (left column) and RI (stimulus-locked, middle and response-locked, right column) averaged over frontal (AFz, F3, Fz, F4, FC1, FCz, FC2) and parietal (C3, Cz, C4, CP1, CPz, CP2) group of electrodes. The lower panel depicts average topographies of the iCNV (0.3–0.6 s) and CNV for SI and RI_{SL} and RI_{RL}, plotted separately for the three durations. The CNV for the left and middle set of topographies is based on the window between 1.5 and 2 s after the onset of the duration, the right most set of topographies depicts response locked topographies averaged over the last 500 ms of the reproduced duration.

longer durations, or more generally a regression towards a (subjective) mean, is typically observed (i.e., Vierordt's Law, e.g., Lejeune and Wearden, 2009) in studies in which multiple intervals are presented in intermixed fashion (e.g., Taatgen and van Rijn (2011)).

4.2. Identification of CNV

Fig. 3 depicts the EEG data observed during the perception and reproduction of the temporal intervals. The left column depicts the development of the CNV during the SI for both a frontal (top row) and a parietal group (second row) of electrodes, with similar plots presented for RI_{SL} and RI_{RL} (middle and right column).

Ramping patterns typical for a CNV can be observed in all plots, and non-parametric cluster-based permutation tests (Maris and Oostenveld, 2007) confirm these patterns. For these CNV analyses, we compared the average amplitude in the time window 0.5 s before the offset of the SI for the SI-based analyses and 0.5 s before the participant-indicated end of the RI (i.e., RI_{RL}) to a baseline defined as the 200 ms before the onset of the SI or RI. All three conditions in SI (2 s: $p=0.001$, for a cluster consisting of AFz, F7, F3, Fz, F4, F8, FC5, FC1, FCz, FC2, FC6, C3, Cz, C4, CP5, CP1, CPz, CP2, CP6, P3, Pz, P4, P8, 3 s; $p=0.002$, for AFz, F7, F3, Fz, F4, F8, FC5, FC1, FCz, FC2, FC6, C3, Cz, C4, CP5, CP1, CPz, CP2, CP6, P3, Pz, P4, P8; 4 s: $p=0.01$, for AFz, F7, F3, Fz, F4, F8, FC5, FC1, FCz, FC2, FC6, C3, Cz, C4, CP5, CP1, CPz, CP2, P3, Pz, P4, P8], and RI_{RL} (2 s: $p=0.006$; for AFz, F7, F3, Fz, F4, F8, FC5, FC1, FCz, FC2, FC6, C3, Cz, C4, CP5, CP1, CPz, CP2, CP6, P3, Pz, P4; 3 s: $p=0.026$, for AFz, F7, F3, Fz, F4, F8, FC5, FC1, FCz, FC2, FC6, C3, Cz, C4, CP5, CP1, CPz, CP2; 4 s: $p=0.043$, for AFz, F7, F3, Fz, F4, F8, FC5, FC1, FCz, FC2, FC6, C3, Cz, C4, CP5, CP1, CP2) showed significant differences between the baseline and the end of the interval. The observed activity in both SI and RI_{RL} and the fronto-central intersection of electrodes is in line with the typical observations in interval timing studies (e.g., Elbert et al., 1991; Gibbons and Rammsayer, 2004; Gibbons and Stahl, 2008; Wiener et al., 2012). The topographies plotted in Fig. 3, showing corresponding topographical distributions of the mean activity during the SI and RI, resemble the typical distribution associated

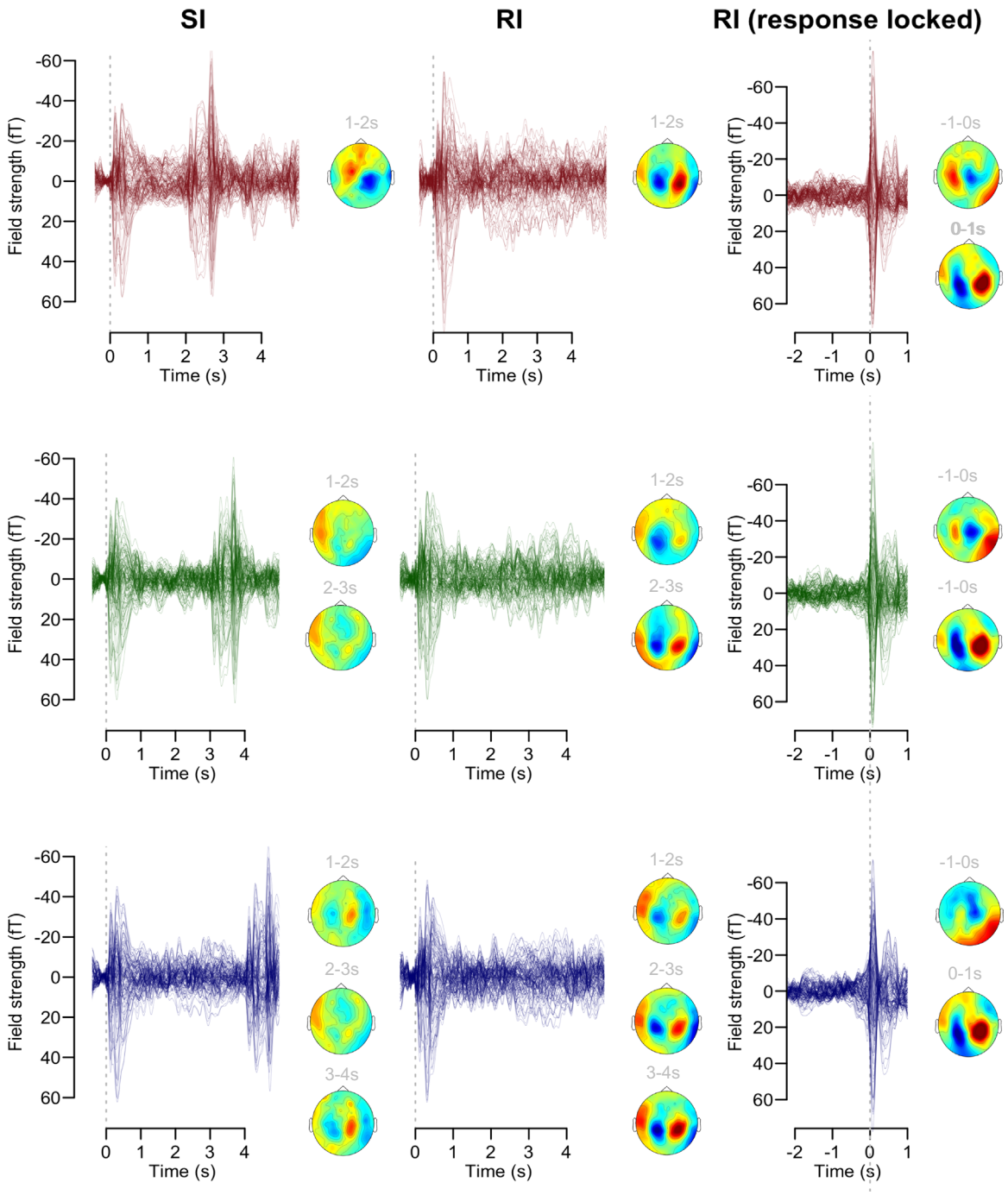

Fig. 4. Each cell represents magnetic fields plotted for all sensors and averaged across all participants for all experimental conditions. Left, middle, and right rows depict the SI stage, RI stage and response locked data in the RI stage, respectively. Topographical plots depict averaged activity as indicated by gray labels (i.e., 1–2 s, 2–3 s, and 3–4 s).

with a CNV (e.g., Boehm et al., 2014).

4.3. Identification of CMV

Fig. 4 shows the MEG data, using the same trials and alignment as used for Fig. 3, with each row representing one duration. Each subfigure contains a plot of all individual sensors because no a-priori subsets of relevant sensors were defined. Visual inspection of the SI MEG data does reveal clear auditory evoked fields, but does not reveal any slow build-up of activity, which should be visible as a divergence of magnetic fields amplitude among the sensors between the two tone bursts. Non-parametric cluster-based permutation tests indeed provided no evidence (all $p > 0.1$) for any differences between the magnetic fields (0.5 s to offset of SI) during the SI stage and the baseline (-0.2 s to onset of SI). Although these results might be slightly different if spatial realignment was performed, the observation of auditory fields indicates that the omission of spatial realignment of the sensor space data is not severely reducing group average fields.

It can be seen in the RI_{SL} data (Fig. 4, middle column) that after an initial peak at around 0.4 s, the magnetic fields return to baseline level and at about 1 s the magnetic fields in all three conditions start to slowly diverge again. Although this cursory inspection of the RI_{SL} data shown in the middle column of Fig. 5 might hint at slow drifting magnetic fields, one should note that a strong field is typically observed in MEG data after a motor

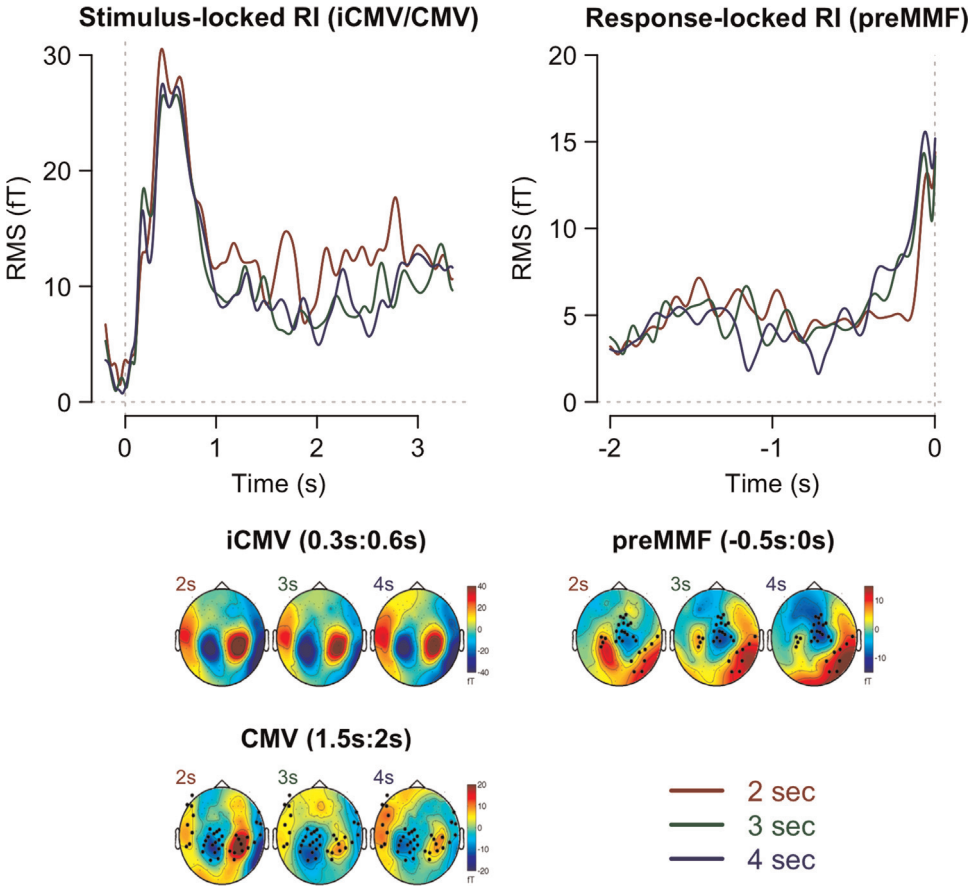

Fig. 5. Sensor-space results for the MEG data. Time courses depict RMS across the MEG sensors significantly different from the baseline interval (marked by bold dots in the topoplots). To identify the most sensitive sensors the data was collapsed over all three conditions and tested against the baseline interval. The left and right panels depict RI_{SL} and RI_{RL} data, respectively. Topoplots depict CMV (1.5–2 s), iCMV (0.3–0.6 s), and preMMF (−0.5 to 0 s) components.

response. This post-movement magnetic field (postMMF) consists of two waves that correspond to reafferent activity and a post-movement positive wave similar to those typically seen in the EEG data (e.g., Praamstra et al., 2003). Given that time reproductions in the RI_{SL} data are distributed around the target duration (see Fig. 2) the increased magnetic fields could have been driven by a jittered postMMF. This interpretation is supported by at least two observations. First, the response locked analyses, shown in the right column of Fig. 4, show that the increase in magnetic fields during the interval is much reduced when the jitter is removed. Second, the similar topographies of the apparent CMV in the RI_{SL} data (Fig. 4, middle column, all topographical plots) and the postMMF in the RI_{RL} data (Fig. 4, right column, right topographical plot), but different RI_{RL} pre-response topographies (Fig. 4, right column, left topographical plot) suggest a common underlying mechanism. To exclude the influence of the postMMF on the observed RI_{SL} data, we decided to limit our analyses to trials with reproduced durations longer than 2 s, and to focus on the interval between 1.5 and 2 s. Running individual analyses per sensor, without taking any repeated testing into account, showed that some sensors were different from the baseline interval. These most-sensitive sensors are depicted in the lower panel of Fig. 5. Although these sensors are quite scattered over the scalp, we calculated a root mean square (RMS) that can be interpreted as overall field strength across given set of sensors. This average field strength for RI_{SL}, depicted in the top-left panel of Fig. 5, shows slight signatures of ramping activity. However, non-parametric cluster-based permutation tests showed that no magnetic fields differed from baseline (−0.2 s to onset of RI) for the conditions (all $p > 0.1$).

Obviously, any RI_{RL} analysis that focuses on data before the response will not be contaminated by a postMMF. Apart from the postMMF, another potential source of contamination are the fields evoked by the tone that signals the onset of the reproduction interval. Therefore, we excluded all trials with reproduced durations shorter than 1.5 s, and focused our RI_{RL} analysis on the last 500 ms of the reproduced interval. This set of criteria results in at least 1 s between the onset of the interval and the start of the analysis window. Non-parametric cluster-based permutation tests showed that the last 500 ms of the RI_{RL} was indeed different from the baseline (−0.2 s to onset of RI) for the three conditions (2 s: positive cluster, $p=0.042$; 3 s: negative cluster, $p=0.005$; 4 s: negative cluster, $p=0.001$; positive cluster, $p=0.085$, where a positive cluster indicates an outflowing field and negative indicates an inflowing field). Fig. 5 depicts the topographies of the magnetic fields, with dots indicating the sensors that are significantly different from the baseline interval (without correction). The time courses of the sensors different from the baseline interval can be seen in the upper-right panel of Fig. 5, with the time courses depicting RMS across the MEG sensors significantly different from the baseline interval (note that all significant sensors, without performing cluster correction, were selected to better depict the time courses of magnetic fields). Indeed, the RI_{RL} plots show a clear buildup that starts around 0.6 s before the response that terminates reproduction interval. Earlier work has linked this pre-movement magnetic field (preMMF) with preparation-based processes (Cheyne et al., 2006).

For better topographical visualization and to determine the source of the observed effects, we reconstructed sources for the data analyzed for RI_{SL} and RI_{RL}. Fig. 6 shows the source reconstructions obtained using LCMV beamformer for both RI_{SL} and

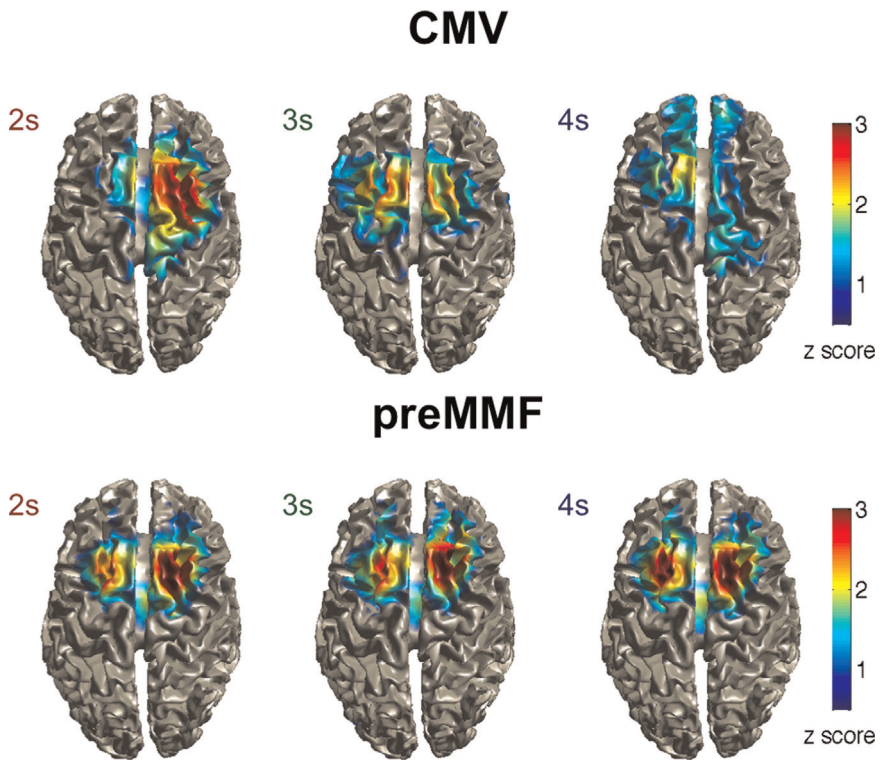

Fig. 6. Source-space results for the MEG data in the RI. Functional data depicts NAI exceeding first standard deviation for the CMV (top row) and preMMF (bottom row).

RI_{RL}. For RI_{SL}, the midfrontal areas are active in the all conditions. However, as the duration becomes longer it can be noticed that activations become less visible. This decrease is likely caused by the smaller contribution of the preMMF activity in the time period ranging from 1.5 to 2 s for longer intervals. Thus, this supports the idea that the CMV-like patterns that might be visible in the RI_{SL} data should be interpreted as a product of dispersed preMMFs.

Source reconstructions for the RI_{RL} did show strong and clear activations (Fig. 6) in the SMA (BA 6) and superior frontal gyrus (BA 6) for all three durations, implicating the involvement of the SMA in the final stages of duration reproduction. This finding is corroborated by the reconstruction of activity specifically generated in the SMA. To construct source space time series, a matrix of beamformer weights was obtained for each subject and subsequently multiplied with a matrix containing sensor space data, with anatomical labels obtained from the Anatomical Automatic Labeling atlas (Tzourio-Mazoyer et al., 2002). Fig. 7, depicting the activity generated from the SMA, shows a steady buildup of activity starting approximately 0.6 s prior to the second key press. This SMA time course closely resembles the SMA dipole time course that was identified by Praamstra et al. (1996, Fig. 4) just before (voluntary) movement.

In sum, the magnetic data does not provide a CNV-like, steady build up of activation that starts at the interval onset as can be observed in the EEG data. However, the MEG data does provide evidence for a preMMF originating from the SMA that builds up about 6 s before the response that indicates the end of the interval is given, most likely reflecting preparatory processes.

4.4. CNV amplitude enhancement for shorter duration

The earlier work by Elbert et al. (1991, cf. Gibbons and Rammsayer, 2004) has shown that the reproductions of shorter intervals were associated with more negative amplitudes, a finding which is at odds with the assumption that the CNV reflects the accumulator. Visual inspection of Fig. 3 (right column) indicates

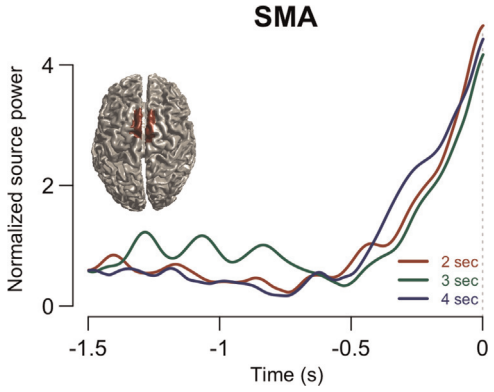

Fig. 7. Normalized source power as obtained in the supplementary motor area. Red region marked on the template brain depicts the SMA label used to obtain beamformer weights. (For interpretation of the references to color in this figure legend, the reader is referred to the web version of this article.)

that also in this study, for both the fronto-central and the centro-parietal CNV, a more negative build-up can be observed for the 2-s condition than for the 3- and 4-s conditions in RI_{SL} and RI_{RL} stages. To quantify this observation, we performed a cluster-based non-parametric permutation test implementing MANOVA *F*-test on the RI_{SL} data for two time periods from 0.3 to 0.6 s (iCNV) and from 1.5 to 2 s (CNV) after the tone indicating the start of RI. We found a significant cluster for the iCNV ($p=0.035$; AFz, F7, F3, Fz, F4, FC5, FC1, FCz, FC2, C3, Cz, CP5, CP1, CPz, CP2, CP6, P7, P3, Pz, P4, P8), and for the CNV ($p=0.045$, AFz, F7, F3, Fz, F4, FC5, FC1, FCz, FC2, C3, Cz, CP5, CP1, CPz, CP2, CP6, P7, P3, Pz, P4, P8). For the RI_{RL} data, cluster-based permutations showed significant differences for the mean activity in last 500 ms of the reproduced interval ($p=0.018$; C3, Cz, CP1, CP2, P3, Pz). No such effects were found for the MEG data (all p values > 0.1).

Both iCNV and CNV topographies (Fig. 3) indicate that 2 s condition is mainly enhanced at the fronto-central sites,

suggesting that response preparation drives the difference between conditions (e.g., Lütcke et al., 2009).

Given that the magnetic data does not provide a CNV-like, steady build up of activation that starts at the interval onset, we did not perform comparison for time period ranging from 1.5 to 2 s. There was no significant difference for the iCMV time interval (0.3–0.6 s) among three RI conditions ($p > 0.1$).

4.5. Slow fields/potentials correlate with interval timing performance

Previous studies have linked CNV to motor preparation (e.g., Loveless and Sanford, 1974). As participants in our study were asked to terminate the reproduction interval by a key press, the CNV measured in the RI is likely to index the level of (motor) preparedness. If CNV and CMV are primarily linked to motor preparation, larger CNV/CMV amplitude should be associated with shorter reproduced intervals as higher level of preparedness should cause faster terminations of the interval. To test this prediction the mean amplitude ranging from 1.5 s to 2 s was taken for every participant and correlated with the average time reproduction (see Fig. 8). To obtain the average CMV and CNV amplitude, all MEG sensors and EEG electrodes that differed from the baseline were used. The CMV data was based on RMS values to prevent from canceling out of inflowing and outflowing magnetic fields. To allow for inclusion of all three reproduction intervals into one model we used linear mixed models (Pinheiro and Bates, 2006). The CNV/CMV amplitude and condition were entered as predictors and subject was used as a random factor and subject was used as a random factor.

Formal model comparisons showed that the CNV amplitude measured during the RI predicts the length of reproduced duration expressed as a ratio between reproduced duration and target duration (note that no evidence was found for the SI CNV amplitude influencing reproduced duration). This conclusion is based on a comparison of a model that includes both RI CNV amplitude and SI duration to a model that only includes an effect of SI duration (2, 3, 4 s). This comparison demonstrated that the inclusion of the CNV amplitude is justified ($\Delta AIC = 4$, $\chi^2_{(1)} = 5.35$, $p = 0.020$), but extending this model with the interaction term between condition and CNV amplitude is not warranted ($\Delta AIC = 4$, $\chi^2_{(2)} = 0.42$, $p = 0.810$). The estimated effect for the CNV amplitude effect was significant ($\beta = 0.022$, $F(1,36.7) = 6.4$, $p = 0.016$, based on a Type 3 ANOVA with Satterthwaite approximation of degrees of freedom), as was the factor encoding SI duration ($F(1,31.6) = 52.5$, $p < 0.001$). Note that the estimated effect for the CNV amplitude is positive, indicating that the more negative the amplitude, the shorter the estimated reproduction – a finding at odds with the hypothesis that the CNV reflects the accumulator.

Although MEG data, shown in the right panel of Fig. 8, resulted in fairly similar slope lines, the individual data points are much more scattered. An analogical model fitting procedure as executed for the CNV data was applied to the MEG data, showing that including the MEG amplitude did not improve the fit ($\Delta AIC = 1.9$, $\chi^2_{(1)} = 0.1$, $p = 0.752$), nor was the inclusion of the interaction between SI duration and CMV warranted ($\Delta AIC = 0.9$, $\chi^2_{(1)} = 3.12$, $p = 0.209$).

In line with the above model comparisons, the estimated effect for MEG amplitude failed to reach significance ($\beta = -0.001$, $F(1, 45.3) = 1.3$, $p = 0.268$), but the condition factor did reach significance ($F(2,32.7) = 46.7$, $p < 0.001$). These numerical differences steam from the fact that the mean reproductions used in the CNV and CMV models differed as trials shorter than 2 s were removed in the previous analyzes of the MEG data to exclude the influence of the postMMF on the RI_{SL} data. All trials were kept for the analysis of the CNV. To assess whether MEG amplitudes might improve the fit of the EEG-based models, we extended the best fitting EEG-model by adding the MEG amplitudes as additional predictor. However, addition of the MEG data to the model containing CNV data was not warranted ($\Delta AIC = 0.7$, $\chi^2_{(2)} = 2.78$, $p = 0.096$). As predicted, the correlation analysis showed that the shorter intervals were associated with larger CNV amplitude. This result is in line with the notion that the CNV amplitude in the reproduction stage indexes the level of preparedness.

4.6. iCNV amplitude correlates with interval timing performance

The EEG data in the RI stage, as depicted in Fig. 3, also shows larger amplitudes for the iCNV when participants reproduced the 2 s interval. This effect suggests that participants initiate preparatory and anticipatory processes right after the first tone onset, or even before the onset of the reproduction interval (Gaillard and Näätänen, 1973; Riehle, 1991; Weinrich et al., 1984). If the iCNV indeed reflects the initial state of preparedness and anticipation, the measured iCNV should predict the length of the reproduced duration more accurately for the short (2 s) duration than for the longer (3 and 4 s) durations. To test this prediction the mean

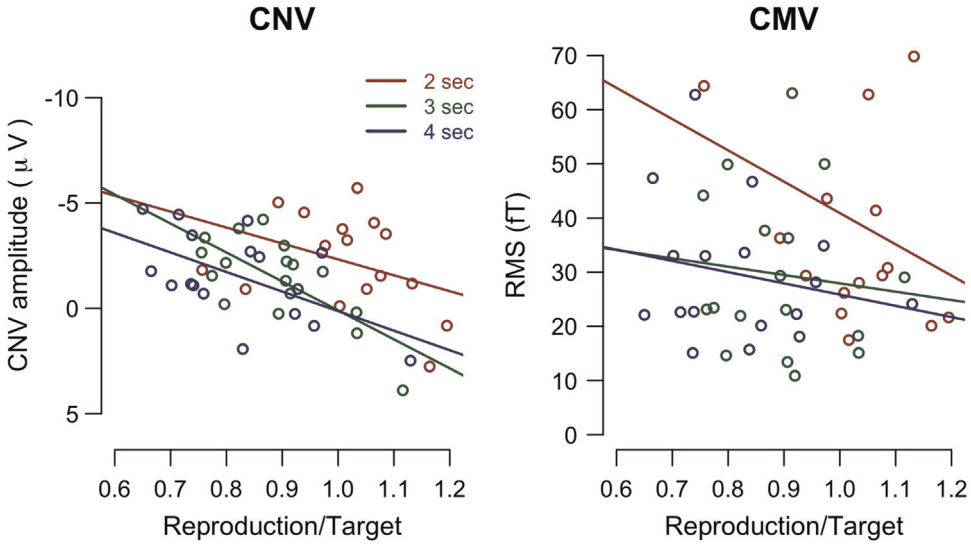

Fig. 8. Correlations between the CNV/CMV amplitude and the length of reproduced interval (expressed as ratio between reproduced and target interval). Each point depicts the CNV/CMV amplitude per participant and per condition.

amplitude ranging from 0.3 s to 0.6 s was calculated per condition for every participant, and we assessed to what extend the amplitude predicts the averaged time reproduction (see Fig. 9). In addition to iCNV amplitude, we also assessed the iCMV amplitude. The average iCMV and iCNV amplitudes are based on all MEG sensors and EEG electrodes that differed from the baseline. As for the CMV analysis, the iCMV data was based on absolute values to prevent that inflowing and outflowing magnetic fields cancel each other out. The iCNV or iCMV amplitude and condition were entered as predictors, subject was used as a random factor, and the average reproduced duration was entered as dependent variable. To assess whether the predictive value of the iCNV amplitude differs per condition, we compared a model that included iCNV amplitude and condition as main effects, and a model that included both main effects and the interaction. The more complex model including interaction term was justified (ΔAIC=2.6, $\chi^2_{(2)}$= 6.55, p=0.038). Closer inspection of the model with the interaction term showed that the estimated effect for the iCNV amplitude under 2 s condition was significant (β=0.64, t(37.2)=3.1, $p < 0.005$). Importantly, in line with the notion that iCNV indexes initial level of preparation at the onset or event before the onset of RI, the estimated effect for the iCNV amplitude under 3 s condition (β=0.015, t(29.4)=2.3, p=0.031) and 4 s (β=0.014, t(28.7)=2.2, p=0.033) condition was lower as compared to 2 s condition. The analyses with iCMV as predictor did not result in any significant effects. Additionally, inclusion of the iCMV data in the model containing iCNV data was not warranted (ΔAIC=0.2, $\chi^2_{(2)}$= 2.17, p=0.141). providing an additional point suggesting that the iCNV and iCMV are functionally different components.

5. Discussion

5.1. Different time courses in CNV and CMV

Although the CNV measured in the encephalogram has been recognized as a signature of the processes involved in interval timing (Elbert et al., 1991; Walter et al., 1964; Ruchkin et al., 1977), both in the context of short (e.g., < 1 s) and long (> 1 s) intervals, the CMV, the magnetic counterpart of the CNV, has not received much attention. The work that has compared the CNV and CMV (N'Diaye et al., 2004), suggests that these measures reflect different properties of interval timing tasks. As these previous studies focused on short intervals, which are often considered to be different from longer intervals, we investigated slow electric potentials and magnetic fields related to supra-second interval timing by co-recording magnetic and electric brain signals. While some studies have shown that the SMA is the main source contributing to CNV (e.g., Gómez et al., 2007), the status of this structure with respect to magnetic activity has not been settled (N'Diaye et al., 2004). To this end, we replicated two classical studies that used the time reproduction paradigm using supra-second durations (Elbert et al., 1991; also see Gibbons and Rammsayer (2004)).

Similarly to the previous work, we obtained a clear ramping activity in the EEG data for both perception (SI) and reproduction (RI) stages. CNV was obtained irrespective of whether trials were averaged in stimulus-locked or response-locked manner, and was maximal at fronto-central locations. These results are in line with the previous work on which this study was based (Elbert et al., 1991; Gibbons and Rammsayer, 2004).

With respect to the MEG data, a more diffuse picture emerged. No magnetic signal related to the encoding of temporal intervals was found. Nevertheless, the SMA and midfrontal structures were involved in the reproduction stage. Although the stimulus locked analysis showed signs of slow rising activity in the MEG data, these effects were absent in the response locked data. For the response locked data we found a magnetic field that starts rising approximately 0.8 s before the key press terminating the timed interval, whereas the response locked CNV starts to build up earlier. As has been suggested by previous work (e.g., Cheyne et al., 2006) this slow magnetic field (termed preMMF) is directly related to late movement preparation. The small effects present in the RI_{SL} might therefore well reflect a smeared preMMF (a hypothesis supported by the similar source reconstructions of the RI_{SL} and RI_{RL} data), and should therefore be interpreted with caution.

As the CMV-like pattern is caused by smeared preMMF and originate from the SMA, this work demonstrates the role of magnetic fields originating from the SMA in the late stages of reproduction of temporal intervals, however this paradigm does not allow to distinguish between SMA involvement in motor preparation and motor timing. At the same time this finding is by no means trivial as the involvement of the SMA in movement generation has been extensively debated (e.g., Praamstra et al., 1996). Factors that could enhance the SMA activity in our paradigm, apart from movement control, of course, could be related to timing and timing related processes (e.g., Baker et al., 2012) as the time reproduction task demands precise timing of movement.

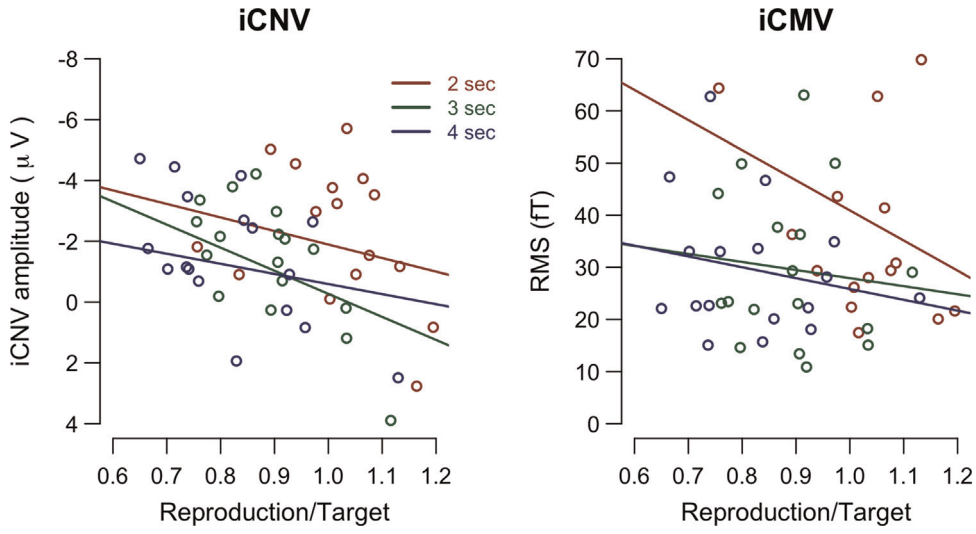

Fig. 9. Correlations between the iCNV/iCMV amplitude and the length of reproduced interval (expressed as ratio between reproduced and target interval). Each single point depicts per participant and per condition iCNV/iCMV amplitude.

Of course, the activation of the SMA in our task is at odds with the results of N'Diaye et al. (2004) who did not find any activation in midfrontal areas. However, as we used a time reproduction task, the observed SMA activity could be partially driven by the response required to end the RI. This interpretation is further supported by the observation that the evidence for sustained activity in the SI stage was much weaker than in the RI stage.

Unlike the MEG data, the EEG data provide a signal that is compatible for RI_{RL} and RI_{SL} averages. This compatibility is manifested by the similarity between RI_{RL} and RI_{SL} time courses and their topographies. Therefore, by means of the difference in morphology of the RI_{RL} and RI_{SL} plots for the EEG and MEG data, the CNV can be interpreted as the continuous signal related to timed interval, whereas the CMV/preMMF signal builds up only prior to the interval termination. If one assumes that the CNV also represents preparatory processes, it is interesting to note that the CNV RI_{RL} data showed a much longer (up to 3 s) buildup (Fig. 3, right column) than the MEG RI_{RL} data. As the preMMF generated in the SMA has been linked to preparatory processes (Praamstra et al., 1996), these results suggest that although both electric and magnetic data might reflect a build up of preparatory processes, the dissimilarity of associated time-frames hints at different aspects of preparation. However, the question remains how these components relate to the timing performance.

5.2. Amplitude of electromagnetic signals and timing behavior

The secondary goal of this study was to investigate how the amplitude of slow electromagnetic fields relates to timing performance as it is typically formalized in terms of the information processing theory of interval timing (Treisman, 1963). This framework has proposed that the pacemaker emits pulses that are integrated by the accumulator, a conceptual account of timing that is the core of many models of interval timing (Gibbon et al., 1984; Taatgen et al., 2007; Van Rijn and Taatgen, 2008). Importantly, this process of accumulation of temporal information, so-called climbing neural activity, has been proposed to be indexed by the slow brain activity that primarily originates from the SMA and is instantiated by the CNV (Macar et al., 1999). What processes are reflected in the CNV, and to what extend they are linked to the conceptual models of interval timing, have recently become a subject of a lively debate (e.g., Tamm et al., 2014; Wittmann 2013; Wiener et al., 2012; Van Rijn et al., 2011). The notion of temporal accumulation predicts that longer intervals should be associated with larger amplitude of the CNV. Strikingly, the CNV amplitude in the RI_{SL} and RI_{RL} data was larger under the 2 s condition than under the 3 s and 4 s conditions. Although the larger amplitude in the 2 s interval in the RI_{SL} data could be caused by the narrower distribution of responses under the 2 s condition, we also found enhanced amplitudes for the 2 s interval in the RI_{RL} data, a finding that cannot be attributed to the wider distributions of time reproductions for longer intervals. This enhanced CNV amplitude is clearly at odds with the notion that the CNV originating from the SMA represents the temporal accumulator (e.g., Herbst et al., 2014; Macar et al., 1999; Wiener et al., 2012; cf., Bueti and Macaluso, 2011; Kononowicz and Van Rijn, 2011; Ng et al., 2011; Wiener and Thompson, 2015). Instead, this work provides additional evidence in support of the notion that the CNV is linked to enhanced preparatory and expectancy processes (Van Rijn et al., 2011). Namely, the absolute CNV amplitude is negatively correlated with reproduced durations across subjects. Importantly, as shown by the model selection, this correlation holds for all the three reproduction durations

The idea that motor preparation explains the enhanced CNV amplitude under the 2 s condition is at odds with previous interpretation of similar decrease in the CNV amplitude for longer intervals (Elbert et al., 1991; cf., Gibbons and Rammsayer, 2004). Elbert et al. (1991) proposed that timing mechanisms for intervals longer than 3 s are different from the timing mechanisms for intervals shorter than 3 s. However, the results of the source localization of the MEG data and topographies of the EEG data do not support that view. Instead, our data suggest that reproduction of temporal intervals might differ in terms of timing of engagement and initiation of preparatory processes as reflected by the CNV. Importantly, our interpretation is in line with the foreperiod studies, demonstrating a decrease in the late component of the CNV amplitude for long intervals (Müller-Gethmann et al., 2003). In the time reproduction task, similarly to the foreperiod paradigm, expectancy can be affected by a decrease in the accuracy of internal timing signal as a temporal interval ages (Gibbon, 1977; Gibbon, 1992; Gibbon et al., 1984). Thus this decreased accuracy of internal timing signal could influence the CNV amplitude via expectancy or changes of temporal uncertainty, both of which are expressed in the modulation of the amplitude of CNA (Trillenberg et al., 2000; Janssen and Shadlen, 2005). These effects, in turn, suggest that the late part of the CNV is not exclusively devoted to motor preparation, but it also exhibits a cognitive-based activity (Baker et al., 2012; Boehm et al., 2014). Summarizing, these studies support the view that many different cognitive systems are involved in the timing of an interval (e.g., Taatgen et al., 2007; Gu et al., (2015)).

Interestingly, a similar line of reasoning holds for the early component (iCNV). The electric data in the RI stage also showed larger amplitude for the iCNV, when participants reproduced the 2 s interval. The enhancement of the iCNV can also be explained, assuming that participants initiate preparatory and anticipatory processes right after the first tone onset or even before the onset of the reproduction interval, something that has been supported using very short foreperiod intervals (Gaillard and Näätänen, 1973). This interpretation is further supported by correlation between iCNV amplitude and reproduced durations across participants. Importantly, we showed that this correlation is significantly stronger in 2 s RI than in the 3 s and 4 s RI, suggesting that on top of the overall amplitude effect there is also a functional difference in how initial iCNV process is utilized. Interestingly, Cui et al. (2009) have found that the signal in the SMA codes for probability of event occurring at the end of a current delay period, and indexes learned expectations. Although the iCNV effects were present at the beginning of temporal interval, it still could reflect updating of expectancy. In our design the beginning of the reproduction interval is preceded by the presentation of the standard interval. The expectancy level at the interval onset and temporal certainty should be higher for the shorter RI, as the preparation level before the start of the interval is larger for shorter intervals (Gaillard and Näätänen, 1973; Riehle, 1991; Weinrich, et al., 1984). Building on that, our results could suggest that the enhancement of the iCNV component is related to the enhanced expectancy for an internal signal that will impact timing of the response (c.f., Kononowicz, 2015).

The CNV that we have found in the RI phase should be distinguished from the SI phase, as these two stages of time reproduction task have different cognitive demands. This is supported by more frontal distribution of the CNV in the SI stage. Frontal activations have been associated with cognitive and anticipatory processes (Brunia, 1988, 1999; Brunia and Van Boxtel, 2001; Leynes et al., 1998). The fMRI studies also localized this anticipatory activity in the frontal regions, especially the inferior frontal gyrus (Coull et al., 2013; Macar, et al., 2006; Wencil et al., 2010). As participants are not required to react in the SI interval, it is unlikely that the buildup is driven by motor preparation. For the MEG data, we did not identify any consistent pattern of ramping activity in the SI stage.

As the setup used in this study does not allow for the reliable

source localization based on the EEG data, further studies should utilize more dense EEG recordings (Acar and Makeig, 2013). Together with MEG signals, they could be utilized for a combined source reconstruction which should significantly increase the spatial precision of sources involved in the interval timing (Palva et al., 2010; Huotilainen et al., 1998). It is also important to consider the type of MEG sensors used. Both the current study and the study by N'Diaye et al. (2004) employed magnetometers. However, Noguchi and Kakigi (2006) used planar gradiometers, which might have allowed them to find slow magnetic shifts. Moreover, in the context of unraveling weak magnetic fields from the SMA and ACC it may be crucial for future studies to obtain individual brain scans that can tremendously improve the accuracy of source reconstruction.

To summarize, in line with N'Diaye's et al. (2004) we found different activity patterns for the CNV and the CMV data, supporting the conclusion that the CNV signal might be a better marker for the investigation of the continuous preparatory processes in interval timing than the CMV. However, the MEG signal may be especially useful and advantageous over the EEG signal when investigating late stages of preparatory and anticipatory (motor) processes, or decisions involved in timing (Gaillard, 1976; Ikeda et al., 1997).

Acknowledgments

This work has been supported by the European Project COST ISCH Action TD0904 (COST 286/09) "Time In Mental activity: Theoretical, behavioral, bioimaging, and clinical perspectives" (TIMELY: www.timely-cost.eu). We thank Udo Boehm for assistance with data acquisition, Nele Russwinkel for assistance with recruiting participants, and Alexandre Gramfort and Robert Oostenveld for the comments on beamforming technique.

References

Acar, Z.A., Makeig, S., 2013. Effects of forward model errors on EEG source localization. Brain Topogr. 26 (3), 378–396.
Baker, K.S., Piriyapunyaporn, T., Cunnington, R., 2012. Neural activity in readiness for incidental and explicitly timed actions. Neuropsychologia 50 (5), 715–722.
Basile, L.F., Rogers, R.L., Bourbon, W.T., Papanicolaou, A.C., 1994. Slow magnetic flux from human frontal cortex. Electroencephalogr. Clin. Neurophysiol. *90* (2), 157–165.
Bell, A.J., Sejnowski, T.J., 1995. An information-maximization approach to blind separation and blind deconvolution. Neural Comput. *7* (6), 1129–1159.
Bender, S., Resch, F., Weisbrod, M., Oelkers-Ax, R., 2004. Specific task anticipation versus unspecific orienting reaction during early contingent negative variation. Clin. Neurophysiol. *115* (8), 1836–1845.
Boehm, U., Van Maanen, L., Forstmann, B., van Rijn, H., 2014. Trial-by-trial fluctuations in CNV amplitude reflect anticipatory adjustment of response caution. Neuroimage *96*, 95–105.
Brunia, B., 1988. Movement and stimulus preceding negativity. Biol. Psychol. *26* (1–3), 165–178.
Brunia, C.H.M., 1999. Neural aspects of anticipatory behavior. Acta Psychol. *101* (2), 213–242.
Brunia, C.H.M., Van Boxtel, G.J.M., 2001. Wait and see. Int. J. Psychophysiol. *43* (1), 59–75.
Buhusi, C.V., Meck, W.H., 2005. What makes us tick? Functional and neural mechanisms of interval timing. Nature Rev. Neurosci. *6* (10), 755–765.
Bueti, D., Macaluso, E., 2011. Physiological correlates of subjective time: evidence for the temporal accumulator hypothesis. NeuroImage *57* (3), 1251–1263.
Cheyne, D., Bakhtazad, L., Gaetz, W., 2006. Spatiotemporal mapping of cortical activity accompanying voluntary movements using an event-related beamforming approach. Hum. Brain Mapp. *27* (3), 213–229.
Coull, J.T., 2009. Neural substrates of mounting temporal expectation. PLoS Biol. *7* (8), e1000166.
Coull, J.T., Davranche, K., Nazarian, B., Vidal, F., 2013. Functional anatomy of timing differs for production versus prediction of time intervals. Neuropsychologia *51* (2), 309–319.
Coull, J.T., Vidal, F., Nazarian, B., Macar, F., 2004. Functional anatomy of the attentional modulation of time estimation. Science *303* (5663), 1506–1508. http://dx.doi.org/10.1126/science.1091573.
Cui, X., Stetson, C., Montague, P.R., Eagleman, D.M., 2009. Ready...Go: amplitude of the fMRI signal encodes expectation of cue arrival time. PLoS Biol. *7* (8), e1000167.
Dammers, J., Ioannides, A.A., 2000. Neuromagnetic localization of CMV generators using incomplete and full-head biomagnetometer. NeuroImage *11* (3), 167–178.
Darvas, F., Pantazis, D., Kucukaltun-Yildirim, E., Leahy, R.M., 2004. Mapping human brain function with MEG and EEG: methods and validation. NeuroImage *23*, 289–S299.
Elbert, T., Rockstroh, B., Hampson, S., Pantev, C., Hoke, M., 1994. The magnetic counterpart of the contingent negative variation. Electroencephalogr. Clin. Neurophysiol./Evoked Potentials Sect. *92* (3), 262–272.
Elbert, T., Ulrich, R., Rockstroh, B., Lutzenberger, W., 1991. The processing of temporal intervals reflected by cnv-like brain potentials. Psychophysiology *28* (6), 648–655.
Fischer, T., Langner, R., Birbaumer, N., Brocke, B., 2008. Arousal and attention: self-chosen stimulation optimizes cortical excitability and minimizes compensatory effort. J. Cognit. Neurosci. *20* (8), 1443–1453.
Fischer, T., Langner, R., Diers, K., Brocke, B., Birbaumer, N., 2010. Temporo-spatial dynamics of event-related EEG beta activity during the initial contingent negative variation. PLoS One *5* (9). http://dx.doi.org/10.1371/journal.pone.0012514.
Gallistel, C.R., Gibbon, J., 2000. Time, rate, and conditioning. Psychol. rev. *107* (2), 289–344.
Gaillard, A.W.K., 1976. Effects of warning-signal modality on the contingent negative variation (CNV). Biol. Psychol. *4* (2), 139–153.
Gaillard, A.W., Näätänen, R., 1973. Slow potential changes and choice reaction time as a function of interstimulus interval. Acta Psychol. *37* (3), 173–186.
Gibbon, J., 1977. Scalar expectancy theory and Weber's law in animal timing. Psychol. Rev. *84* (3), 279–325.
Gibbon, J., 1992. Ubiquity of scalar timing with a poisson clock. J. Math. Psychol. *36* (2), 283–293.
Gibbon, J., Church, R.M., Meck, W.H., 1984. Scalar timing in memory. Ann. NY Acad. Sci. *423* (1), 52–77.
Gibbons, H., Rammsayer, T.H., 2004. Current-source density analysis of slow brain potentials during time estimation. Psychophysiology *41* (6), 861–874.
Gibbons, H., Stahl, J., 2008. ERP predictors of individual performance on a prospective temporal reproduction task. Psychol. Res. *72* (3), 311–320.
Gómez, C.M., Marco, J., Grau, C., 2003. Preparatory visuo-motor cortical network of the contingent negative variation estimated by current density. NeuroImage *20* (1), 216–224.
Gómez, C.M., Fernández, A., Maestú, F., Amo, C., Gonzalez-Rosa, J.J., Vaquero, E., Ortiz, T., 2004. Task-specific sensory and motor preparatory activation revealed by contingent magnetic variation. Cognit. Brain Res. *21* (1), 59–68.
Gómez, C.M., Flores, A., Ledesma, A., 2007. Fronto-parietal networks activation during the contingent negative variation period. Brain Res. Bull. *73* (1–3), 40–47.
Gu, B.-M., van Rijn, H., Meck, W.H., 2015. Oscillatory multiplexing of neural population codes for interval timing and working memory. Neurosci. Biobehav. Rev. *48*, 160–185.
Haggard, P., 2008. Human volition: towards a neuroscience of will. Nat. Rev. Neurosci. *9* (12), 934–946.
Hari, R., Levänen, S., Raij, T., 2000. Timing of human cortical functions during cognition: role of MEG. Trends Cognit. Sci. *4* (12), 455–462.
Hämäläinen, M., Hari, R., Ilmoniemi, R.J., Knuutila, J., Lounasmaa, O.V., 1993. Magnetoencephalography—theory, instrumentation, and applications to noninvasive studies of the working human brain. Rev. Mod. Phys. *65* (2), 413.
Herbst, S.K., Chaumon, M., Penney, T.B., Busch, N., 2014. Flicker-induced time dilation does not modulate EEG correlates of temporal encoding. Brain Topogr., 1–11.
Hillebrand, A., Singh, K.D., Holliday, I.E., Furlong, P.L., Barnes, G.R., 2005. A new approach to neuroimaging with magnetoencephalography. Hum. Brain Mapp. *25* (2), 199–211.
Hultin, L., Rossini, P., Romani, G.L., Högstedt, P., Tecchio, F., Pizzella, V., 1996. Neuromagnetic localization of the late component of the contingent negative variation. Electroencephalogr. Clin. Neurophysiol. *98* (6), 435–448.
Ikeda, A., Shibasaki, H., Kaji, R., Terada, K., Nagamine, T., Honda, M., Kimura, J., 1997. Dissociation between contingent negative variation (CNV) and bereitschaft-spotential (BP) in patients with parkinsonism. Electroencephalogr. Clin. Neurophysiol. *102* (2), 142–151.
Janssen, P., Shadlen, M.N., 2005. A representation of the hazard rate of elapsed time in macaque area LIP. Nat. Neurosci. *8* (2), 234–241.
Keil, J., Weisz, N., Paul-Jordanov, I., Wienbruch, C., 2010. Localization of the magnetic equivalent of the ERN and induced oscillatory brain activity. NeuroImage *51* (1), 404–411.
Kononowicz, T.W., Van Rijn, H., 2011. Slow potentials in time estimation: the role of temporal accumulation and habituation. Front. Integr. Neurosci. *5* (48).
Kononowicz, T.W., van Rijn, H., 2014. Decoupling interval timing and climbing neural activity: a dissociation between CNV and N1P2 amplitudes. J. Neurosci. *34* (8), 2931–2939.
Liu, Y., Zhang, D., Ma, J., Li, D., Yin, H., Luo, Y., 2013. The attention modulation on timing: an event-related potential study. PLoS One *8* (6), e66190.
Lewis, P.A., Miall, R.C., 2003. Distinct systems for automatic and cognitively controlled time measurement: evidence from neuroimaging. Curr. Opin. neurobiol. *13* (2), 250–255.
Lejeune, H., Wearden, J.H., 2009. Vierordt's the experimental study of the time sense (1868) and its legacy. Eur. J. Cognit. Psychol. *21* (6), 941–960.

Leuthold, H., Sommer, W., Ulrich, R., 2004. Preparing for action: Inferences from CNV and LRP. J. Psychophysiol. *18* (2), 77–88.
Leynes, P.A., Allen, J.D., Marsh, R.L., 1998. Topographic differences in CNV amplitude reflect different preparatory processes. Int. J. Psychophysiol. *31* (1), 33–44.
Loveless, L., Sanford, S., 1974. Slow potential correlates of preparatory set. Biol. Psychol. *1* (4), 303–314.
Lütcke, H., Gevensleben, H., Albrecht, B., Frahm, J., 2009. Brain networks involved in early versus late response anticipation and their relation to conflict processing. J. Cognit. Neurosci. *21* (11), 2172–2184.
Macar, F., Vidal, F., 2003. The CNV peak: an index of decision making and temporal memory. Psychophysiology *40* (6), 950–954.
Macar, F., Vidal, F., 2004. Event-related potentials as indices of time processing: a review. J. Psychophysiol. *18* (2–3), 89.
Macar, F., Vidal, F., 2009. Timing processes: an outline of behavioural and neural indices not systematically considered in timing models. Can. J. Exp. Psychol. *63* (3), 227–239.
Macar, F., Coull, J., Vidal, F., 2006. The supplementary motor area in motor and perceptual time processing: FMRI studies. Cognit. Process. *7* (2), 89–94.
Macar, F., Vidal, F., Casini, L., 1999. The supplementary motor area in motor and sensory timing: evidence from slow brain potential changes. Exp. Brain Res. *125* (3), 271–280.
Mackert, B.-M., Wübbeler, G., Burghoff, M., Marx, P., Trahms, L., Curio, G., 1999. Non-invasive long-term recordings of cortical 'direct current'(DC–) activity in humans using magnetoencephalography. Neurosci. Lett. *273* (3), 159–162.
Maris, E., Oostenveld, R., 2007. Nonparametric statistical testing of EEG- and meg-data. J. Neurosci. Methods *164* (1), 177–190.
Mento, Tarantino, Sarlo, G.A., Bisiacchi, V.A., M.A., Silvia, P., 2013. Automatic temporal expectancy: a high-density event-related potential study. PLoS One *8* (5), e62896.
Mento, G., Tarantino, V., Vallesi, A., & Silvia, P., (2014). Spatiotemporal Neurodynamics Underlying Internally and Externally Driven Temporal Prediction: A High Spatial Resolution ERP Study.
Müller-Gethmann, H., Ulrich, R., Rinkenauer, G., 2003. Locus of the effect of temporal preparation: evidence from the lateralized readiness potential. Psychophysiology *40* (4), 597–611.
Nachev, P., Kennard, C., Husain, M., 2008. Functional role of the supplementary and pre-supplementary motor areas. Nat. Rev. Neurosci. *9* (11), 856–869.
Nagai, Y., Critchley, H.D., Featherstone, E., Fenwick, P.B.C., Trimble, M.R., Dolan, R.J., 2004. Brain activity relating to the contingent negative variation: an fmri investigation. NeuroImage *21* (4), 1232–1241.
N'Diaye, K., Ragot, R., Garnero, L., Pouthas, V., 2004. What is common to brain activity evoked by the perception of visual and auditory filled durations? a study with MEG and EEG co-recordings. Brain Res. Cognit. Brain Res. *21* (2), 250–268.
Ng, K.K., Tobin, S., Penney, T.B., 2011. Temporal accumulation and decision processes in the duration bisection task revealed by contingent negative variation. Front. Integr. Neurosci. *5* (77).
Noguchi, Y., Kakigi, R., 2006. Time representations can be made from nontemporal information in the brain: an MEG study. Cereb. Cortex *16* (12), 1797–1808.
Nolte, G., 2003. The magnetic lead field theorem in the quasi-static approximation and its use for magnetoencephalography forward calculation in realistic volume conductors. Phys. Med. Biol. *48* (22), 3637.
O'Connell, R.G., Dockree, P.M., Robertson, I.H., Bellgrove, M.A., Foxe, J.J., Kelly, S.P., 2009. Uncovering the neural signature of lapsing attention: electrophysiological signals predict errors up to 20s before they occur. J. Neurosci. *29* (26), 8604–8611.
Oostenveld, R., Fries, P., Maris, E., Schoffelen, J.-M., 2011. FieldTrip: open source software for advanced analysis of MEG, EEG, and invasive electrophysiological data. Comput. Intell. Neurosci. *2011*, 1–12.
Palva, J.M., Monto, S., Kulashekhar, S., Palva, S., 2010. Neuronal synchrony reveals working memory networks and predicts individual memory capacity. Proc. Nat. Acad. Sci. *107* (16), 7580–7585.
Penfield, W., Welch, K., 1951. The supplementary motor area of the cerebral cortex: a clinical and experimental study. Arch. Neurol. Psychiatry *66* (3), 289.
Pinheiro, J., Bates, D., 2006. Mixed-effects Models in S and S-PLUS. Springer Science & Business Media.
Pouthas, V., Garnero, L., Ferrandez, A.M., Renault, B., 2000. ERPs and PET analysis of time perception: spatial and temporal brain mapping during visual discrimination tasks. Hum. Brain Mapp. *10* (2), 49–60.
Praamstra, P., Kourtis, D., Kwok, H.F., Oostenveld, R., 2006. Neurophysiology of implicit timing in serial choice reaction-time performance. J. Neurosci.: Off. J. Soc. Neurosci. *26* (20), 5448–5455.
Praamstra, P., Stegeman, D.F., Horstink, M.W.I.M., Cools, A.R., 1996. Dipole source analysis suggests selective modulation of the supplementary motor area contribution to the readiness potential. Electroencephalogr. Clin. Neurophysiol. *98* (6), 468–477.
Praamstra, P., Turgeon, M., Hesse, C.W., Wing, A.M., Perryer, L., 2003. Neurophysiological correlates of error correction in sensorimotor-synchronization. NeuroImage *20* (2), 1283–1297.
Rammsayer, T.H., 1999. Neuropharmacological evidence for different timing mechanisms in humans. Q. J. Exp. Psychol.: Sect. B *52* (3), 273–286.
Riehle, A., 1991. Visually induced signal-locked neuronal activity changes in precentral motor areas of the monkey: hierarchical progression of signal processing. Brain Res. *540* (1), 131–137.
Robinson, S.E., Vrba, J., 1999. Functional neuroimaging by synthetic aperture magnetometry (SAM).. In: Yoshimoto, T., et al. (Eds.), Recent Advances in Biomagnetism. Tohoku University Press, Sendai, pp. 302–305.
Ruchkin, D.S., McCalley, M.G., Glaser, E.M., 1977. Event related potentials and time estimation. Psychophysiology *14* (5), 451–455.
Sander, T.H., Leistner, S., Wachs, M., Burghoff, M., Curio, G., Mackert, B.M., & Trahms, L., 2009, January. Recording of DC-MEG and peripheral signals in stroke patients. In: World Congress on Medical Physics and Biomedical Engineering, September 7–12, 2009, Munich, Germany, Springer, Berlin, Heidelberg, pp. 222–224.
Scheibe, C., Ullsperger, M., Sommer, W., Heekeren, H.R., 2010. Effects of parametrical and trial-to-trial variation in prior probability processing revealed by simultaneous electroencephalogram/functional magnetic resonance imaging. J. Neurosci. *30* (49), 16709–16717.
Sieroka, N., Dosch, H.G., Specht, H.J., Rupp, A., 2003. Additional neuromagnetic source activity outside the auditory cortex in duration discrimination correlates with behavioural ability. NeuroImage *20* (3), 1697–1703.
Simons, R.F., Öhman, A., Lang, P.J., 1979. Anticipation and response set: cortical, cardiac, and electrodermal correlates. Psychophysiology *16* (3), 222–233.
Sheather, S.J., Jones, M.C., 1991. A reliable data-based bandwidth selection method for kernel density estimation. J. R. Stat. Soc. Ser. B (Methodological), 683–690.
Taatgen, N., van Rijn, H., 2011. Traces of times past: representations of temporal intervals in memory. Memory Cognit. *39* (8), 1546–1560.
Taatgen, N.A., van Rijn, H., Anderson, J.R., 2007. An integrated theory of prospective time interval estimation: the role of cognition, attention, and learning. Psychol. Rev. *114* (3), 577–598.
Tamm, M., Uusberg, A., Allik, J., Kreegipuu, K., 2014. Emotional modulation of attention affects time perception: evidence from event-related potentials. Acta Psychol. *149*, 148–156.
Tanji, J., 1994. The supplementary motor area in the cerebral cortex. Neurosci. Res. *19* (3), 251–268.
Tecce, J.J., 1972. Contingent negative variation (CNV) and psychological processes in man. Psychol. Bull. *77* (2), 73–108.
Todorovic, A., van Ede, F., Maris, E., de Lange, F.P., 2011. Prior expectation mediates neural adaptation to repeated sounds in the auditory cortex: an MEG study. J. Neurosci. *31* (25), 9118–9123.
Treisman, M., 1963. Temporal discrimination and the indifference interval: Implications for a model of the "internal clock". Psychol. Monogr.: Gen. Appl. *77* (13), 1–31.
Trillenberg, P., Verleger, R., Wascher, E., Wauschkuhn, B., Wessel, K., 2000. CNV and temporal uncertainty with 'ageing' and 'non-ageing' S1-S2 intervals. Clin. Neurophysiol. *111* (7), 1216–1226.
Tzourio-Mazoyer, N., Landeau, B., Papathanassiou, D., Crivello, F., Etard, O., Delcroix, N., Joliot, M., 2002. Automated anatomical labeling of activations in SPM using a macroscopic anatomical parcellation of the MNI MRI single-subject brain. NeuroImage *15* (1), 273–289.
Ulrich, R., Leuthold, H., Sommer, W., 1998. Motor programming of response force and movement direction. Psychophysiology *35* (6), 721–728.
Van Rijn, H., Gu, B.-M., Meck, W.H., 2014. Dedicated clock/timing-circuit theories of time perception and timed performance. Adv. Exp. Med. Biol. *829* (5), 75–99.
Van Rijn, H., Kononowicz, T.W., Meck, W.H., Ng, K.K., Penney, T.B., 2011. Contingent negative variation and its relation to time estimation: a theoretical evaluation. Front. Integr. Neurosci. 5 (48).
Van Rijn, H., Taatgen, N.A., 2008. Timing of multiple overlapping intervals: how many clocks do we have? Acta Psychol. *129* (3), 365–375.
Van Veen, B.D., Van Drongelen, W., Yuchtman, M., Suzuki, A., 1997. Localization of brain electrical activity via linearly constrained minimum variance spatial filtering. IEEE Trans. Biomed. Eng. *44* (9), 867–880.
van Wassenhove, V., Lecoutre, L., 2015. Duration estimation entails predicting when. NeuroImage *106*, 272–283.
Verleger, R., Wauschkuhn, B., van der Lubbe, R., Jaśkowski, P., Trillenberg, P., 2000. Posterior and anterior contribution of hand-movement preparation to late CNV. J. Psychophysiol. *14* (2), 69–86.
Vieth, J., Fenwick, P.B.C., Grummich, P., Lumsden, J., Kober, H., Fenton, G.W., Weise, E., 1991. First observations on the magnetic contingent negative variation (CMV) recorded by a multichannel system. Biomed. Tech./Biomed. Eng. *36* (1), 153–154.
Walter, W.G., Cooper, R., Aldridge, V.J., McCallum, W.C., Winter, A.L., 1964. Contingent negative variation: an electric sign of sensori-motor association and expectancy in the human brain. Nature *203*, 380–384.
Wencil, E.B., Coslett, H.B., Aguirre, G.K., Chatterjee, A., 2010. Carving the clock at its component joints: neural bases for interval timing. J. Neurophysiol. *104* (1), 160–168.
Weinrich, M., Wise, S.P., Mauritz, K.H., 1984. A neurophysiological study of the premotor cortex in the rhesus monkey. Brain *107* (2), 385–414.
Wiener, M., Thompson, J.C., 2015. Repetition enhancement and memory effects for duration. NeuroImage *113*, 268–278.
Wiener, M., Kliot, D., Turkeltaub, P.E., Hamilton, R.H., Wolk, D.A., Coslett, H.B., 2012. Parietal influence on temporal encoding indexed by simultaneous transcranial magnetic stimulation and electroencephalography. J. Neurosci. *32* (35), 12258–12267.
Wiener, M., Turkeltaub, P., Coslett, H.B., 2010. The image of time: a voxel-wise meta-analysis. NeuroImage *49* (2), 1728–1740.
Wittmann, M., 2013. The inner sense of time: How the brain creates a representation of duration. Nat. Rev. Neurosci. *14* (3), 217–223.